Mechanical and Corrosion Performance of Inorganic Hollow Spherical Microparticle-Epoxy Composite Coatings

Ananthapadmanabhan S. Sreenivasan, [1] Tapan K. Rout, [2] Smrutiranjan Parida 1 *
1Indian Institute of Technology Bombay, Mumbai- 400076, India.
[2 Tata] Steel Limited, Jamshedpur- 831001, India.
*Email id: paridasm@iitb.ac.in

Abstract: Organic coatings are used as a protective barrier against the corrosion and natural oxidation of metal substrates. Mechanical integrity is also an important aspect of durability. Epoxy based coatings are the most widely used coating systems on metal substrates. In this study, an epoxy composite coating with hollow spherical (HSP) microparticles was investigated for anti-corrosion and mechanical properties. Using an economical surface treatment of HSP microparticles an enhanced mechanical property with high adhesion (5B), high hardness (8H) and impact strength of up to 15 J was achieved. The corrosion performance of the coating was very good from the electrochemical impedance spectroscopy. However, with the increasing loading of the treated HSP microparticles, a decrease in the corrosion resistance due to low packing effect was observed. On the other hand, on prolonged exposure to the corrosion medium, a performance decrease has been observed. The electrochemical impedance study and the salt spray test in 5 wt% NaCl solution concurred on the same result. However, there is a clear advantage in the thermal insulation character of the coating which is indicated by a 27% and 15% decrease in temperature, respectively, with respect to the uncoated and simple epoxy coating on the metal substrate of 1mm thickness. The apparent decrease away from the surface was more than this. From the sustainability point, this economical material is beneficial for external coating applications on the structures requiring high integrity, corrosion performance and temperature moderation.

Keywords: Composite coating, Hardness, Impact, Adhesion,

1. Introduction

Various metallic structures in public places can be coated with organic coatings which can provide better mechanical integrity, and corrosion protection. Organic coatings are known to improve durability and other particular technical characteristics [1, 2]. Epoxy-based coatings are the most widely used coating systems for corrosion protection of steel structures under diverse atmospheric conditions, because of its remarkable chemical resistance, electrical insulating qualities, and strong adhesion to heterogeneous metal surfaces [3, 4]. Therefore, these coatings are used in a wide range of applications especially as primers [5-7]. Various inorganic fillers are used in the epoxy to mitigate their vulnerability to mechanical damage and weathering failures [8-10]. Their poor mechanical durability stems mainly from the extremely low cross-linked structure and the presence of unsaturated bonds in the structure [11]. These flaws in the epoxy coating may serve as pathways for water, oxygen, and aggressive species to enter the coating and reach the coated metallic substrate quickly, initiating localized corrosion [12-14]. The added fillers of various length scales in the epoxy composite coatings are used to increase the protectiveness of the epoxy coatings not only by mitigating the flaws in the matrix but also increase the barrier performance [15,16]. The influences of size, volume fraction, and degree of dispersion of the fillers on the mechanical response of polymer composites [17] have been investigated to show that smaller fillers are better for yield strength of the coatings, but their role in influencing the adhesion of the coating to the metal substrate needs more investigation as no correlation to the size was found from the literature [18]. However, there are reports on the increase in the adhesion to the resin matrix by the functionalization of the fillers [19, 20]. Additionally, in epoxy coatings, the size of the reinforcing fillers

has been found to increase its barrier performance by reducing porosity and zigzagging the diffusion channel for harmful species [18, 21, 22]. While nanomaterials display very good filler performance, they are often expensive [23] and cannot be consistently prepared with the same qualities [24, 25]. In this case use of easily available inexpensive materials can be considered for valuable reuse giving better sustainability [26-30]. However, in such cases, their worthiness in coating application must be investigated.

The present study is an attempt in this direction for the HSP microparticles, where the corrosion performance, and mechanical properties of the epoxy-HSP composite coatings were evaluated. The epoxy systems usually lack impact strength and hardness when applied thickness is <100 μm. This study gives insight into the reasons for failure and the advantages in the coating properties. Besides, value addition in the thermal insulation is shown in millimeter thin metallic substrates. This study shows the worthiness of the coating for applications on rooftops, equipment parts, vehicle compartments, etc. In the present study, a facile direct incorporation processing method for treated HSP microparticles into the epoxy to get optimum dispersion and enhances the coating performances is reported.

MATERIALS AND METHODS

Materials

The epoxy resin and hardener (Korrtek Top 381/ Hard 300) used in this study were obtained from Leotek Innovations, Mumbai, India. The epoxy resin was a multifunctional low molecular weight diglycidyl ether of bisphenol A. The hardener belongs to the class of an aliphatic amine. The epoxy resin and the hardener were mixed in a 1:1 (wt./wt.) proportion. The HSP microparticles of 10-100 μm size made up of aluminosilicate were used which were supplied by Kulin Corporation (Nagpur, India). Xylene and sodium chloride were obtained from Merck (USA).

Coating formulation

Firstly, the HSP microparticles were washed thoroughly in DI water with agitation sequentially using a homogeniser and then ultrasonicator, and then filtered and dried in a hot air oven. For surface modification, the dried HSP microparticles were treated with ethanol for 30 minutes by agitation in a homogeniser, then washed in DI water, filtered, and dried in a hot air oven at 105°C. Desired quantity of treated HSP microparticles (5, 10, 15, and 20 wt% with respect to the resin) was added to the resin along with the solvent thinner and homogenised using a high shear homogeniser (at 3000 rpm) for a period of 30 minutes. To this mixture, the hardener was added in the prescribed ratio (1:1) and mixed using a magnetic stirrer at 1000 rpm for a period of 20 minutes. The composite coating was applied on mild steel panels of size 3 x 6 inches of 1 mm thickness, which were previously polished using emery paper of grade 100 to 1200 to remove rust and other impurities from the surface, and then cleaned using acetone. The prepared coatings formulation was applied to these cleaned substrates using a bar applicator. The coatings were cured in a dry place at room temperature for 7 days to get the appropriate coatings. The dry film thickness of the coating was 65±5 μm.

Characterization techniques

The surface of the HSP microparticles before and after the ethanol treatment was studied by using Fourier Transform Infrared (FTIR) Spectroscopy using Perkin Elmer Spectrum GXA FTIR spectrometer in the wave number range of 4000-400 cm^{-1}. The crystalline phases in HSP microparticles were investigated using an X-ray diffractometer (SHIMADZU, XRD-6100) with Copper (Cu) Kα radiation (λ = 1.5406 Å) at a current of 30 mA at 40 kV. The continuous scanning was carried out in the 5 to 90° 2θ range with a 10° minute-1 scan speed. The morphology of the HSP microparticles was observed using a scanning electron microscope (Hitachi S3400). The samples were sputter coated with carbon to avoid the charging effect caused by the nonconductive nature of the HSP microparticles.

Evaluation of Mechanical Properties

In the study, cross-hatch adhesion, pull-off adhesion, hardness, and impact strength were measured in order to evaluate the effect of HSP microparticles on the mechanical performance of the coatings with various wt.% of HSP microparticles. Cross-hatch adhesion tests (ASTM D3359) were

performed by making a lattice pattern with six cuts in perpendicular directions on the coated substrate. A pressure-sensitive tape was glued over the cut and then pulled out, and adhesion was then evaluated by comparing the pattern with the standard illustrations. Pull-off adhesion tests (ASTM D4541) were performed by sticking a dolly normal to the coating surface using glue (Araldite standard epoxy adhesive). After the glue was cured, the testing apparatus was attached to the dolly and the force applied was gradually increased till, either the dolly was detached, or a specified load value was reached, when the test was terminated. Pencil hardness tests were performed as per ASTM D3363 standard by scratching the coating surface with pencils of increasing hardness. During the test, the pencil was mounted to press down on the paint surface at an angle of 45° and with a load of 750 grams. The hardness range of pencils used was from 9B to 9H. Impact resistance (ASTM D2794) was measured by dropping a standard (indenter) weight from a given distance, after hitting indented the coating. After the impact, the deformed impact area of the coating was probed for cracks or delamination.

Corrosion resistance study

Corrosion performance of the coatings was studied using electrochemical impedance spectroscopy (EIS) and neutral salt spray test. EIS was performed using a potentiostat and a three-electrode electrochemical cell, in which the coated panel was the working electrode, saturated calomel electrode (SCE) was the reference electrode and a platinum wire mesh was the counter electrode. A 3.5 wt% NaCl was used as the electrolyte in the EIS study. The PGSTAT 30 Autolab (Metrohm) potentiostat with the FRA was used for EIS measurement. The EIS measurement was carried in frequency range 100 kHz to 10 mHz with an amplitude of 10 mV. All EIS measurements were performed at the room temperature. For long-term corrosion study, the EIS was performed on each coating in the interval of every 24 hrs, which ended at 720 hrs. The EIS data were analysed using analysis software in the potentiostat. Salt spray tests of coated panels were performed in a salt spray cabinet, as per ASTM B117. The salt spray was executed at an air pressure of 1.1 to 1.3 bar at the nozzle. The salt solution was made by dissolving 5 ± 1 parts by weight of sodium chloride in 95 parts of demineralized water. The temperature in the cabinet was maintained at 35 ± 2 °C. St. Andrews 'X' cuts were made on the coated panels with a 1 mm scratch tool (Cutter), which were exposed for a period of 720 hrs. The exposed coatings were tested for blistering, corrosion progress and adhesion loss.

Study of the temperature shielding

The temperature shielding effect of the coating was studied by measuring temperature differences at the opposite surface of the coated panel fitted in a model insulated wooden box and the test panels were placed on the roof as shown in Figure 1. An infrared lamp of 150 W was used as the source of IR light, which was placed 30 cm away from the test panel's exposed surface. Four thermal sensors were placed at an advantageous position for recording the temperature at different locations inside the wooden box, as shown in Figure 1; one is on the top of the panel for measuring the input temperature and another three were behind exposed panels and insides the box. The temperature readings were recorded at 30 minutes intervals from which the temperature differences were calculated.

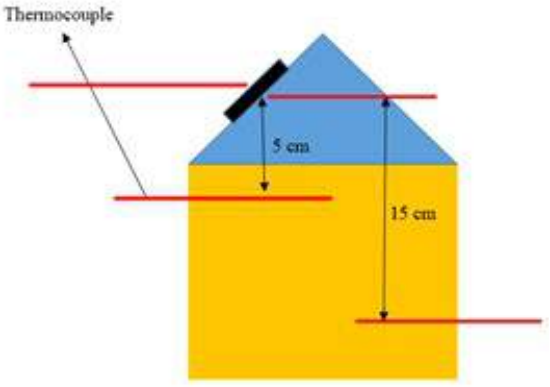


Fig. 1. Schematic design of the set-up used to measure thermal insulation property of coating.

RESULTS AND DISCUSSION

Spatial, phase and surface chemical nature of HSP microparticles

The surface modification of the HSP microparticles was intended to increase the bonding through the

generation of functional groups and surface roughness [31, 32]. FTIR analysis helped to evaluate the functional modification on the surface of the treated HSP microparticles. FTIR spectrum of the untreated (uHSP) and treated HSP (tHSP) microparticles in Figure 2a showed an increase in the peak at 3440 cm^{-1} associated with the vibration of the hydroxyl group (–OH) in the treated HSP. This stems from the alcoholic treatment of the HMS. The HSP microparticles also contained two major bands which are characteristic internal vibrations peaks of TO_4 tetrahedra (T = Al, Si), appearing at 1081 cm^{-1} and 457 cm^{-1} corresponding to the symmetric and asymmetric T-O stretching vibrations, which have also increased in the treated HSP microparticle. The peak at 511 cm^{-1} corresponds to Ti-O vibrations, unchanged due to treatment.

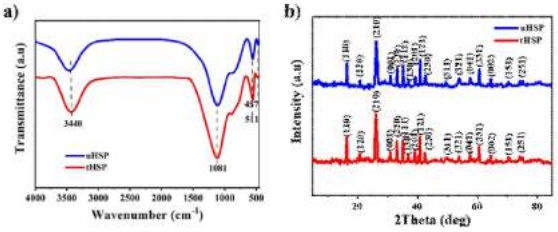


Fig. 2. (a) FTIR spectrum of MS and treated HSP microparticles, (b) XRD spectrum of uHSP and tHSP microparticles.

XRD patterns of untreated and treated HSP microparticles, Figure 2b, shows the typical phases present in these particles [33, 34]. The results reveal that the HSP microparticles are mainly composed of the crystalline phase of mullite (JCPDS file no. 79-1456) in addition to the main amorphous glassy phase. The surface treatment procedure with ethanol is not expected to cause any change in the crystal structure of HSP microparticles.

The surface morphology of the untreated and treated HSP microparticles was observed in the SEM images as shown in Figure 3. The HSP microparticles were spherical with an average size of 25 µm (particle size ranging between 10-100 µm). The particles were well separated from each other, hence no agglomeration. After the treatment with ethanol, the surface of treated HSP microparticles developed a little smoothness due to the etching action in the ultrasonic condition used during the treatment.

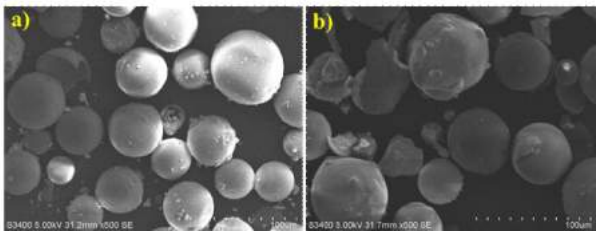


Fig. 3. SEM images of (a)uHSP and (b)tHSP microparticles

Mechanical Properties of the coatings

HSP microparticles have an average particle size of 25 µm with a wide size distribution ranging between 10-100 µm. The effect of the size and wide distribution in size on the mechanical performance of the epoxy- HSP microparticles composite coating was evaluated by performing adhesion tests using cross hatch and pull-off adhesion test techniques. The results of these tests are presented in Table 1 and Figure 4a. For bare epoxy coating, the cross-hatch adhesion strength confirms to 3B grade, corresponding to an exfoliation rate of nearly 30%. Upon incorporation of treated HSP microparticle fillers, the adhesion strength is found to increase with the increase in the filler content. At 20 wt% treated HSP microparticle loading, the adhesion strength increased to a 5B rating corresponding to an exfoliation rate of less than 5%. This trend in adhesion was also confirmed by the pull-off adhesion test. The pull-off adhesion strength of the composite coating increased from 1.67 MPa in bare epoxy to 3.73 MPa in the composite coating with 20 wt% treated HSP microparticles. The treated HSP microparticles improved the adhesion strength of the coating, which can be attributed to the formation of a –Si-O-Fe (Fe = metal substrate) bond with the substrate through the surface bonds present in the treated HSP microparticles [35], as inferred from the FTIR result. Observing the pulled-out region, it is found that the failures are primarily adhesive, not cohesion failure. This indicated very good interfacial bonding with the epoxy matrix [36, 37], which further justified the role of abundant –OH functional groups in adhesion.

The hardness of the coatings was measured using the pencil hardness test with pencil grade varying from 9B to 9H and results are shown in Table 1. For the bare epoxy composite coating, the hardness was confirmed to 6H grade as per the ASTM standard. The pencil hardness of the composite coating

improved with the increase in the treated HSP microparticle content, and at 20 wt% of treated HSP microparticles, a maximum pencil hardness of 8H was observed. The indenter had to interact with more filler particles as the treated HSP microparticle number increased in the coating. In addition, the well-dispersed treated HSP microparticles in the epoxy limit the molecular chain mobility in the matrix, contributing to the increased pencil hardness [38, 39]. The impact resistance of the epoxy composite coating also increased with the increase in the treated HSP microparticles content, indicated by the increasing impact energy absorbed by the coating as noted in Figure 4b. The impact resistance of the coating increased from 8.60 J to 15.18 J upon increasing the treated HSP microparticle content from 0 wt% to 20 wt%, respectively. The improved impact resistance is attributed to the very good interaction of treated HSP microparticles with the epoxy resin facilitated by the high concentration of functional groups on the surface of the treated HSP microparticles ensuring better dispersion. Better dispersion of the treated HSP microparticles helps distribute the impact energy uniformly and limits the molecular chain mobility of the epoxy binder [40, 41].

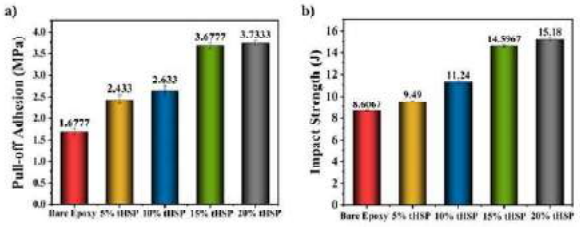


Fig. 4. Mechanical properties of coatings (a) pull-Off adhesion, (b) impact strength of epoxy-treated HSP composite coatings.

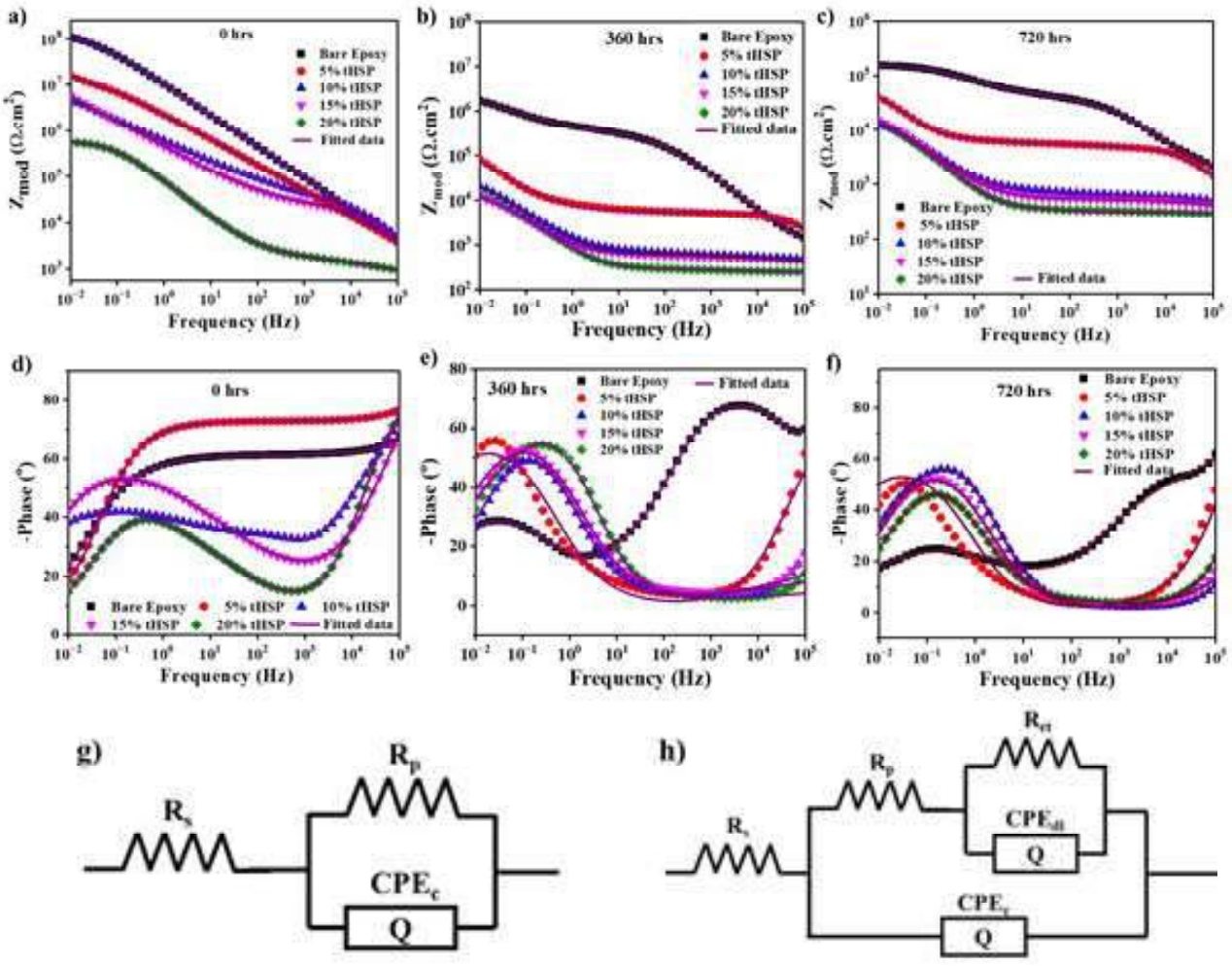


Figure 5: EIS modulus plot ((a), (b), (c)), Bode plot ((d), (e), (f)) of epoxy-treated HSP composite coatings on long term immersion in 3.5 wt% NaCl solution. Equivalent Circuit models for fitting the EIS results (g) in the early-stage analysis, (h) prolonged immersion stage analysis.

Table 1: Cross hatch and pencil hardness of the epoxy-treated HSP composite coatings

Coating System	Cross-hatch Adhesion	Pencil Hardness
Bare Epoxy	3B	6H
5% tHSP microparticles	3B	7H
10% tHSP microparticles	4B	7H
15% tHSP microparticles	4B	8H
20% tHSP microparticles	5B	8H

Corrosion performance of the coatings

The corrosion resistance of the composite coatings was assessed by the EIS technique by exposing the coated panel to 3.5 wt% salt (NaCl) solution for a period of 30 days. The EIS data were fitted with suitable equivalent circuits (Figure 5) from which the useful polarization resistance was determined, which is an indicator of the corrosion resistance [36, 42, 43]. The corrosion resistance value of the coating system was evaluated and noted in Table 2. At the beginning of the immersion (0 hours, i.e., immediately after immersion), the simplified Randles equivalent circuit, Figure 5g, well describes the system (except 20 wt% system), in which R_s is the solution resistance, R_p is the coating resistance and CPE_c is the nonideal coating capacitance or the layer capacitance (Figure 5a). Immediately after the immersion (0 h, Figures 5a & 5d) the Bode plot also shows a single-time constant matching to the equivalent circuit used for the fitting. As the immersion time progressed, the electrolyte penetrated the system and the coating started to degrade. At this point (360 to 720 h) the entire system can be represented by the equivalent circuit shown in Figure 5h, representing two-time constants, where new parameters the CPE_{dl} and Rct correspond to the charge transfer resistance of newly formed interface with the metal. Based on the nature of the EIS response, a suitable equivalent circuit were used for fitting the data and calculation of corrosion resistance.

The analysis of EIS Bode plots, Figure 5, showed that, compared to the neat epoxy coating, the corrosion resistance of the composite coatings decreased with the increase in treated HSP microparticles in the epoxy (Table 2). The resistance value at the lowest frequency after different hours of exposure was obtained after fitting with the appropriate equivalent circuit (Fig. 5 g, h) as tabulated in Table 2. Similar analyses are frequently used for evaluation of coating corrosion as found in many literature reports [44-46, 29]. At a given exposure time the coating resistance of the coating decreased with the increase in treated HSP microparticles in the epoxy. Similarly, for a given composite coating with a fixed treated HSP microparticle, the corrosion resistance decreased with the increase in the exposure time. With addition of 5% treated HSP microparticles the Rct value is decreased to $1.18 \times 10^7\ \Omega.cm^2$ from $1.52 \times 10^8\ \Omega.cm^2$ at the initial phase of immersion. After 720 hrs of

Table 2: Corrosion resistance of coating samples at different time of immersion to 3.5 wt% NaCl solution

Coating System	Corrosion Resistance ($\Omega.cm^2$)		
	0 hrs	**360 hrs**	**720 hrs**
Bare Epoxy	1.52×10^8	2.47×10^6	2.09×10^5
5% tHSP microparticles	1.18×10^7	3.21×10^5	7.59×10^4
10% tHSP microparticles	5.24×10^6	1.80×10^5	2.44×10^4
15% tHSP microparticles	1.42×10^6	5.24×10^4	2.24×10^4
20% tHSP microparticles	9.12×10^5	4.84×10^4	1.82×10^4

immersion in 3.5 wt% NaCl solution the Rct value for bare epoxy and 5% treated HSP microparticles were $2.09x10^5$ $\Omega.cm^2$ and $7.59x10^4$ $\Omega.cm^2$ respectively. Upon further increase in treated HSP microparticles to 20% the Rct value decreased to $9.12x10^5$ $\Omega.cm^2$ at 0 hrs of immersion and $1.82x10^4$ $\Omega.cm^2$ after 720 hrs of immersion. The decrease in the corrosion resistance can be attributed to the large average particle size of the treated HSP microparticle fillers, resulting in interstitial porosity in the regions between particles. These pores can form the access path for the corrosive medium in the coating layer and result in corrosion of the metal substrate [26, 27, 47, 48]. The corrosion resistance drops with the immersion time, as for the longer exposure water diffusion into the coating increases. Eventually, this speeds up the corrosion of the metal substrate.

The corrosion resistance performance of coatings obtained by the EIS studies was in good agreement with the salt spray test. The results obtained from the salt spray test after 500 h exposure are presented in Figure 6 and Table 3. On analyzing the coating surface after 500 h salt spray exposure, in the bare epoxy and composite coatings with treated HSP microparticles showed small blisters. In composite coatings blistering increased with the increase in the loading (5 to 20 wt%) of treated HSP microparticles in the coating, where medium-sized blisters in large density were formed (Figure 6(a-e)). With the increase in the treated HSP microparticle content, the porosity in the composite coating was also increased due to its large particle size, and the increased porosity resulted in corrosion by the penetration of the salt solution. In all the cases there was no delamination of the coatings indicating better adhesion than discussed in the previous section. The adhesion strength of composite coating after the exposure decreased due to corrosion (Figure 6(f-j)). The delaminated coating surface, after adhesion, showed undercoating corrosion propagation in some epoxy-treated HSP microparticles composite coating (with 10% loading).

Table 3: Salt spray test analysis and adhesion on the exposed epoxy-treated HSP coatings

Coating System	Blister	Adhesion strength
Bare Epoxy	8, M	6
5% treated HSP microparticles	6, M-D	6
10% treated HSP microparticles	6, M-D	4
15% treated HSP microparticles	6, D	4
20% treated HSP microparticles	6, D	2

Adhesion Rating: 10- Best, 0- Worst. **Blister Rating:** 2- large blister, 8- small blister, 10- No blister, F- few, M- medium, D- dense

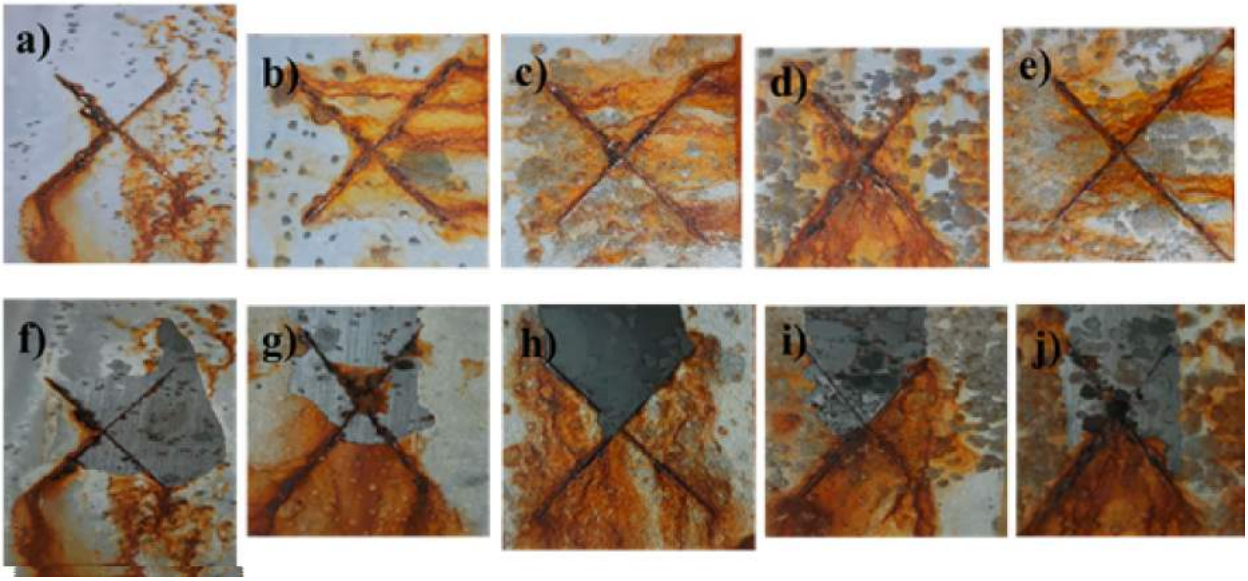


Figure 6: Surface condition of different epoxy-treated HSP coatings after salt spray test for 500 hours, (a) Bare epoxy, (b) 5% treated HSP microparticles, (c) 10% treated HSP microparticles, (d) 15% treated HSP microparticles, (e) 20% treated HSP microparticles, and corresponding images after the adhesion test on exposed coatings (f – j), respectively, Bare epoxy, and composite coatings with 5%, 10%, 15% and 20% treated HSP microparticle)

Exposure to heat for temperature shielding

The temperature shielding properties of the coatings were examined by exposing them to an infrared (IR) source in a custom-built apparatus (Fig. 1). The temperature difference at different distances from the surface was used to determine the temperature shielding properties of the coated panels. Figure 7 demonstrates that after 180 minutes of exposure to infrared (IR) light, the composite coatings with treated HSP microparticles resulted in a greater decrease in temperature compared to the uncoated steel and the epoxy-coated panel. As depicted in Figure 7, a composite coating containing 15% treated HSP microparticles exhibited a temperature decrease of 13 °C just below the panel and 15 °C at 15 cm below the panel when compared to bare steel (Fig. 7 a & b). The lower thermal conductivity of the HSP microparticles act as barrier for the transmission of heat through the coating and hence the showing good temperature shielding property.

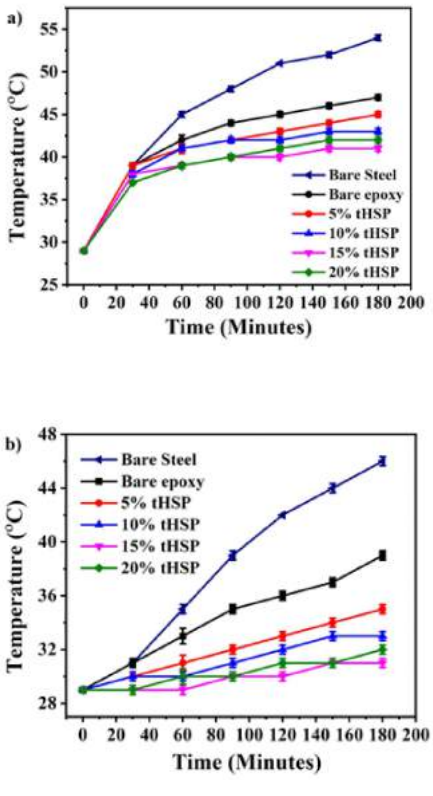


Figure 7: Time vs temperature of epoxy-treated HSP microparticles coatings a) bottom surface of coated plate, b) 15 cm below the coated panel and inside the box.

CONCLUSIONS

The treated HSP microparticle fillers were incorporated into an epoxy resin and their mechanical, corrosion, and temperature shielding properties were investigated. The treated HSP microparticles significantly enhanced the coating's mechanical and thermal performance. The uniform dispersion of treated HSPs resulted in the dissipation of impact energy, resulting in significantly enhanced impact resistance. Corrosion results from the EIS and salt spray study indicated a notable lack of improvement. While good interfacial bonding with the resin and possibly the metal improves mechanical performance, the large size of the treated HSP microparticles causes interstitial porosity in the coating and degrades its corrosion resistance. Thus, the treated HSP microparticle fillers can be utilised to improve the coating's mechanical properties. To increase corrosion resistance, it is plausible to use another filler with a smaller particle size to decrease its interstitial porosity and boost its barrier property. Additionally, modification with longer chain functional groups may be investigated.

ACKNOWLEDGMENTS

The authors acknowledge with gratitude IIT Bombay and TATA Steel, Jamshedpur, for supporting this work financially and providing the research facilities.

REFERENCES

[1] Talbert R. (2004), "Paint technology handbook", CRC Press, Taylor & Francis group.

[2] Paul S. (1995), "Surface Coatings: Science and Technology", 2nd edition.

[3] Deng F., Wang L., Zhou Y., Gong X., Zhao X., Hu T. and Wu C. (2017), "Effect of nanosilica content on the corrosion inhibition of composite coatings of a filled epoxy resin grafted with a hydrophobic fluoroalkylsilane: a dual critical concentrations interpretation", RSC advances, Vol. 7, pp. 48876–48893

[4] Jeon H., Park J. and Shon M. (2013), "Corrosion protection by epoxy coating containing multi-walled carbon nanotubes",

Journal of Industrial and Engineering Chemistry, Vol. 19, pp. 849–853

[5] Galliano F. and Landolt D. (2002), "Evaluation of corrosion protection properties of additives for waterborne epoxy coatings on steel", Progress in Organic Coatings, Vol. 44, Issue 3, pp. 217-225.

[6] Lee H. and Neville K. (1967), "Handbook of epoxy resin", McGraw-Hill, 1st edition

[7] Isik I., Yilmazer U. and Bayram G. (2003), "Impact modified epoxy/montmorillonite nanocomposites: synthesis and characterization", Polymer, Vol. 44, Issue 20, pp. 6371-6377.

[8] Wetzel B., Haupert F. and Zhang M. Q. (2003), "Epoxy nanocomposites with high mechanical and tribological performance", Composites Science and Technology 63, pp. 2055–2067.

[9] Ji W.F., Li C.W., Huang W. J., Yu H. K., Chen R. D., Yu Y. H., Yeh J. M., Tang W. C., and Su Y. C. (2020), "Degradation of epoxy coatings cooperated with polyaniline nanowires in the outdoor environment", Polymers Advanced Technologies, Vol. 32, Issue 3, pp. 988-999.

[10] Li Z., Wang F., Lai Y., Shi Z., Yu Y. (2021), "Flexible epoxy graphene thermoset with excellent weather and corrosion resistance", Progress in Organic Coatings, Vol.151, 106052

[11] Yamini S., Young R. J. (1977), "Stability of crack-propagation in epoxy-resins", Polymer 18 pp. 1075–1080.

[12] Shi X., Nguyen T. A., Suo Z., Liu Y. and Avci R. (2009), "Effect of nanoparticles on the anticorrosion and mechanical properties of epoxy coating", Surface and Coatings Technology, Vol. 204, Issue 3, pp. 237-245.

[13] Wei Y.H., Zhang L.X. and Ke W. (2007), "Evaluation of corrosion protection of carbon black filled fusion-bonded epoxy coatings on mild steel during exposure to a quiescent 3% NaCl solution", Corrosion Science, Vol. 49, pp. 287–302

[14] Pourhashem S., Ghasemy E., Rashidi A. and Vaezi M. R. (2018), "Corrosion protection properties of novel epoxy nanocomposite coatings containing silane functionalized graphene quantum dots", Journal of Alloys and Compounds, Vol. 731, pp. 1112-1118

[15] Al-Turaif H. A. (2010), "Effect of nano TiO2 particle size on mechanical properties of cured epoxy resin", Progress in Organic Coatings, Vol. 69, Issue 3, pp. 241-246.

[16] Allahverdi A., Ehsani M., Janpour H. and Ahmadi S. (2012), "The effect of nanosilica on mechanical, thermal and morphological properties of epoxy coating", Progress in Organic Coatings, Vol. 75, Issue 4, pp. 543-548.

[17] Conardi M., Kocijan A., Kek-Merl D., Zorko M. and Verpoest I. (2014), "Mechanical and anticorrosion properties of nanosilica-filled epoxy-resin composite coatings", Applied Surface Science 292, pp. 432–437.

[18] Ananthapadmanabhan S. S., Mishra G. and Parida S. (2022), "A Review on Corrosion, Adhesion, and Anti-Microbial Performance of Epoxy-Based Nanocomposite Coatings", In: Kamachi Mudali, U., Subba Rao, T., Ningshen, S., G. Pillai, R., P. George, R., Sridhar, T.M. (eds) A Treatise on Corrosion Science, Engineering and Technology. Indian Institute of Metals Series. Springer, Singapore, pp. 423-446.

[19] Thi T. N., Mai T. D., Thi N. P., Thu P. N., Hai V. V. T. and Quang M. N. (2019), "Enhanced Anti-Corrosion Protection of Carbon Steel with Silica-Polypyrrole-Dodecyl Sulfate Incorporated into Epoxy Coating", Journal of Electronic materials, Vol. 48(6), pp. 3931-3938.

[20] Atta A. M., Ahmed M. A., Tawfek A. M. and El-Faham A. (2020), "functionalization of silica with triazine hydrazide to improve corrosion protection and interfacial adhesion properties

of epoxy coating and steel substrate", coatings Vol. 10, 351

[21] Lamaka S. V., Zheludkevich M. L., Yasakau K. A., Serra R., S.K. Poznyak S. K. and Ferreira M. G. S. (2007), "Nanoporous titania interlayer as reservoir of corrosion inhibitors for coatings with self-healing ability", Progress in Organic Coatings 58, pp. 127–135.

[22] Daradmare S., Raj S., Bhattacharyya A. R. and Parida S. (2018), "Factors affecting barrier performance of composite anti-corrosion coatings prepared by using electrochemically exfoliated few-layer graphene as filler", Composites Part B, Vol.155, pp. 1–10

[23] Zurutuza A., Marinelli C. (2014), "Challenges and opportunities in graphene commercialization", Nature Nanotech Vol. 9, pp. 730–734.

[24] Whitener Jr. K. E. and Sheehan P. E. (2014), "Graphene synthesis", Diamond and Related Materials, Vol. 46, pp. 25-34

[25] Lin L., Peng H. and Liu Z. (2019), "Synthesis challenges for graphene industry", Nature materials, Vol. 18, pp. 520–524.

[26] Hu Y., Zhang H., Cheng X, Li F. and Chen T. (2011), "Electroless plating of silver on cenosphere particles and the investigation of its corrosion behavior in composite silicon rubber", Applied Surface Science, Vol. 257, Issue 7, pp. 2813-2817.

[27] Saravanan V., Thyla P., Nirmal N. and Balakrishnan S. (2015), "Corrosion Behavior of Cenosphere -Aluminium Metal Matrix Composite in Seawater Condition". International Journal of ChemTech Research, Vol. 8, pp. 726-731.

[28] Ramezanzadeh B. and Attar M. M. (2011), "Studying the corrosion resistance and hydrolytic degradation of an epoxy coating containing ZnO nanoparticles", Materials Chemistry and Physics, Vol. 130, Issue 3, pp. 1208-1219.

[29] Liu T., Liu Y., Ye Y., Li J., Yang F., Zhao H. and Wang L. (2019, "Corrosion protective properties of epoxy coating containing tetraaniline modified nano-α-Fe2O3", Progress in Organic Coatings, Vol. 132, pp. 455-467.

[30] Zor S. and Ilmieva N. (2018), "Corrosion behavior of PANI/Epoxy/nano SnO2 polymeric nanocomposite coated stainless steel in 3.5 wt% NaCl", Polymer composites, Vol. 39, Issue 54, pp. 2415-2425.

[31] Matin E., Attar M. M. and Ramezanzadeh B. (2015), "Investigation of corrosion protection properties of an epoxy nanocomposite loaded with polysiloxane surface modified nanosilica particles on the steel substrate", Progress in Organic Coatings, Vol. 78, pp. 395-403

[32] Liu Y., Xia C., Zehri A., Ye L., Wang N., Zhmud B., Lu H. and Liu J. ((2019), "Surface Modification of Graphene for Use as a Structural Fortifier in Water-Borne Epoxy Coatings", Coatings, Vol. 9, Issue 11, 754.

[33] Yu X., Shen Z. and Xu Z. (2007), "Preparation and characterization of Ag-coated cenospheres by magnetron sputtering method", Nuclear Instruments and Methods in Physics Research B, Vol. 265, pp. 637–640.

[34] Meng X., Shen X. and Liu W. (2012), "Synthesis and characterization of Co/cenosphere core–shell structure composites", Applied Surface Science, Vol. 258, Issue 7, pp 2627-2631.

[35] Bakhshandeh E., Jannesari A., Ranjbar Z., Sobhani S. and Saeb M. R. (2014), "Anti-corrosion hybrid coatings based on epoxy–silica nano-composites: Toward relationship between the morphology and EIS data", Progress in Organic Coatings vol. 77, pp. 1169–1183.

[36] Haddadi S. A., Ramazani S. A. A., Mahdavian M., Taheri P. and Mol J. M. C. (2019), "Mechanical and Corrosion Protection Properties of a Smart Composite Epoxy Coating with Dual-Encapsulated Epoxy/

Polyamine in Carbon Nanospheres", Industrial & Engineering Chemistry Research, Vol. 58, pp. 3033-3046.

[37] Rajabi M., Rashed G. R. and Zaarei D. (2015), "Assessment of graphene oxide/ epoxy nanocomposite as corrosion resistance coating on carbon steel", Corrosion Engineering, Science and Technology, Vol. 50, Issue 9, pp. 509-516.

[38] Jasim K.A., Fadhil R. N., Shaban H.A., Jaafar H. I., Maiyaly B. K. H., Aleabi S. H. and Salman E. M. (2019), "The effects of copper additives on the glass transition temperature and hardness for epoxy resin", Progress in Industrial Ecology – An International Journal, Vol. 13, No. 2, pp. 163-172.

[39] Liu F. and Guo K. (2014), "Reinforcing epoxy resin through covalent integration of functionalized graphene nanosheets", Polymers for Advanced Technologies, Vol. 25, Issue 4, pp. 418-423.

[40] Fadl A. M., Abdou M.I., Al-Elaa S. A., Hamza M. A. and Sadeek S.A. (2019), "Evaluation the anti-corrosion behavior, impact resistance, acids and alkali immovability of nonylphenol ethoxylate/TiO hybrid epoxy nanocomposite coating applied on the carbon steel surface", Progress in Organic Coatings, Vol. 136, 105263

[41] Zaarei D., Sarabi A. A., Sharif F., Gudarzi M. M. and Kassiriha S. M. (2010), "The Impact of Organoclay on the Physical and Mechanical Properties of Epoxy-Clay Nanocomposite Coatings", Journal of Macromolecular Science, Part B, Vol. 49, Issue 5, pp. 960-969.

[42] Wang C., Liu S., Li M., Wang Z., Luo H., Fan W., Liu Z. and Liu F. (2021), "Novel Environmentally Friendly Waterborne Epoxy Coating with Long-Term Antiscaling and Anticorrosion Properties", Langmuir, Vol. 37, pp. 9439-9450.

[43] Xie Y., Liu C., Liu W., Liang L., Wang S., Zhang F., Shi H. and Yang M. (2020), "A novel approach to fabricate polyacrylate modified graphene oxide for improving the corrosion resistance of epoxy coatings", Colloids and Surfaces A: Physicochemical and Engineering Aspects, Vol. 593, 124627.

[44] Palraj S., Selvaraj M., Maruthan K., Rajagopal G. (2015), "Corrosion and wear resistance behavior of nano-silica epoxy composite coatings", Progress in Organic Coatings, Vol. 81, pp. 132–139.

[45] Lv X., Li X., Zhang H., Zheng Y., Wu J., Tao X. (2019), "ZrO2 nanoparticle encapsulation of graphene microsheets for enhancing anticorrosion performance of epoxy coatings", Surface & Coatings Technology, Vol. 358, pp. 443–451.

[46] Raj X. J. (2017), "Application of EIS and SECM Studies for Investigation of Anticorrosion Properties of Epoxy Coatings Containing Zinc Oxide Nanoparticles on Mild Steel in 3.5% NaCl Solution", Journal of Materials Engineering and Performance, Vol. 26, pp. 3245–3253.

[47] Mandal D. P., Majumdar D. D., Bharti R. K. and Majumdar J. D. (2015), "Microstructural characterisation and property evaluation of titanium cenosphere syntactic foam developed by powder metallurgy route", Powder Metallurgy, 58:4, pp. 289-299.

[48] Ahamed A. and Prashanth T. (2016), "Corrosion behaviour of cenosphere aluminium 6061 composites", International Journal of Advanced Materials Manufacturing and Characterization, 6, pp. 64-68.